The effect of deposition conditions on adhesion strength of Ti and Ti6Al4V cold spray splats

Goldbaum, Dina; Shockley, J. Michael; Chromik, Richard R.; Rezaeian, Ahmad; Yue, Stephen; Legoux, Jean-Gabriel; Irissou, Eric

Publisher's version / Version de l'éditeur:
https://doi.org/10.1007/s11666-011-9720-3
Journal of Thermal Spray Technology, 21, 2, pp. 288-303, 2012-03-01

The effect of deposition conditions on adhesion strength of Ti and Ti6Al4V cold spray splats.

Dina Goldbaum, J. Michael Schockley, Richard R. Chromik, Ahmad Rezaeian, Stephen Yue, Jean-Gabriel Legoux and Eric Irissou.

Abstract

Cold spray is a complicated process where many parameters have to be considered in order to achieve ideal material deposition. In cold spray process deposition velocity influences the degree of material deformation and material adhesion. While most materials can be easily deposited at relatively low deposition velocity (<700m/s), this is not the case for high yield strength materials like Ti and its alloys. In the present study, we evaluate the effect of deposition velocity, powder size, particle position in the gas jet, gas temperature and substrate temperature on the adhesion strength of cold spayed Ti and Ti6Al4V splats. A micromechanical test technique was used to shear individual splats of Ti or Ti6Al4V and measure their splat adhesion strength. The splats were deposited onto Ti or Ti6Al4V substrates over a range of deposition conditions with either nitrogen or helium as the propelling gas. The splat adhesion testing coupled with microstructural characterization was used to define the strength, the type and the continuity of the bonded interface between splat and substrate material. The results demonstrated that optimization of spray conditions makes it possible to obtain splats with high adhesion strength close to the shear strength of Ti and continuously bonded interface. Splats of either material studied, that had high adhesion strength, had some combination of the following characteristics: they were of the smaller size range (< 20 μm diameter), found along the center of the deposition pass, sprayed at very high velocity, or onto a pre-heated substrate. It was also found that for Ti6Al4V, high adhesion strength was only observed at higher deposition conditions compared to Ti. Through comparisons made to literature, a good correlation was found between the splat adhesion strength and particle cohesion strength in the coatings.

Introduction

The cold spray process is based on numerous principles of gas flow, material deformation and thermodynamics [1]. The coating deposition is achieved with a de-Laval type nozzle, where pressurized and preheated nitrogen or helium gas undergoes compression and expansion imparting supersonic velocities to the feed-stock powders [1]. The particle velocity at which deposition takes place is known as critical velocity. At critical velocity, high stress fluctuation in the material lead to plastic deformation and a formation of adiabatic shear instability region [2]. In the adiabatic shear instability region, temperature approached and can even reach the melting point of material. The increase in the flow stresses and temperature results in a formation of a conformal interface and some extent of metallurgical bonding [3-5].

The critical velocity is a function of the material yield strength and temperature, and is different for different materials [2]. For Ti and Ti alloys the critical velocity can be as high as 700 to 900m/s [2, 6]. The particle velocity with respect to the critical velocity and the temperature of the impacting particles and the substrate can play an important role on the cold spray deposition. Experimental studies have shown that a good correlation exists between the

particle deposition velocity, particle deformation and adhesion [7, 8]. The particles that undergo extensive deformation and adhere to the substrate material are often referred to as splats. The generally accepted model of the cold spray splat deposition mechanisms as function of particle velocity is illustrated in Figure 1 [2, 3, 5, 8, 9].

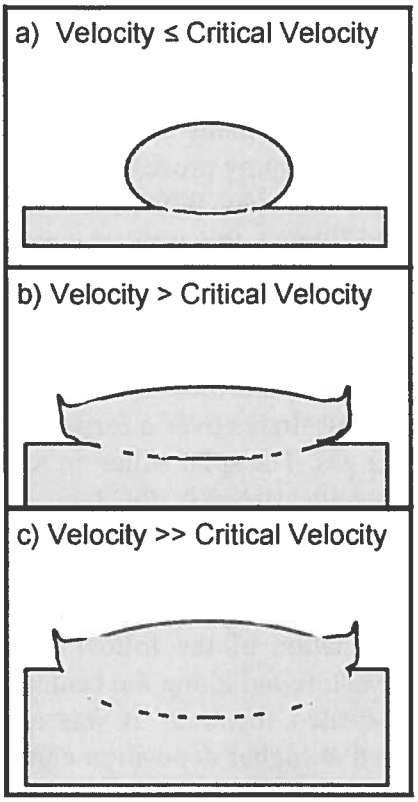

Figure1: General appearance of cold sprayed splats as a function of particle velocity with respect to the critical velocity. This figure is a summary of current understanding of the cold spray process based on the references cited in the body of this paper. It is generalized and the three regimes can change when one changes the splat or substrate material or changes the temperature. When the particle velocity is low (a), deformation takes place, but very little adiabatic shear. At medium particle velocities (b), there is significant deformation of the splat and formation of adiabatic shear and metallurgical bonding in these local regions. However, the substrate remains undeformed. At the highest particle velocities (c), both the splat and substrate deform extensively and a combined adiabatic shear process leads to an increase in the length of the conformal interface and an increase in the density of regions that have become metallurgically bonded.

Three types of splat deformation behaviour have been reported [1, 7-11]. At the deposition velocity below or approaching the critical velocity, the material undergoes plastic deformation that is measured as a function of splat width divided by the splat height and referred to as splat flattening ratio or FR [4, 7, 12]. At the impacting velocity below the critical velocity, the transition to the adiabatic shear instability is limited and results in limited metallurgical bonding if any [2, 3, 6]. For that reason, the bonding between the splat and the substrate is mostly through a weak conformal adhesion resulting from mechanical interlocking of asperities.

Figure 1a illustrates this deposition mode. As the deposition velocity surpasses the critical velocity, Figure 1b, the formation of the adiabatic shear instability becomes more pronounced leading to a material jetting and increase in FR. The formation of adiabatic shear instability and increase in the splat substrate interface leads to a greater fraction of the interface being metallurgically bonded and a stronger splat adhesion [3, 8]. Another type of the deposition behaviour is often observed for splats deposited at velocities significantly higher than the critical velocity. The deformation takes place not only in the cold sprayed materials but also in the substrate material and contributes to a splat-substrate interface of even greater extent with more metallurgical bonding and even stronger splat adhesion as can be seen in Figure 1c [9, 13].

A number of particle impact simulations have been used to understand the deposition mechanisms of metals like copper and aluminum onto copper or aluminum, as well as titanium and its alloys onto steel and titanium substrates [2-4, 6, 9, 13-15]. The deposition velocity was shown to have a significant effect on the particle deformation [7] and adhesion [8, 9] but was also predicted to affect the temperature rise in the adiabatic shear instability region [3, 6, 9]. Recent studies indicate that while particle velocity plays a major role in cold spray deposition process, other parameters such as particle impact temperature [16] and substrate temperature [17] may also affect the cold spray deposition process [1, 8]. Higher impact temperature of the splats or substrate lowers the critical velocity required for the cold spray deposition [6] and was shown to contribute to a better splat adhesion to a substrate material as well as to the particle cohesion strength in the coating [8, 18]. Particle and substrate temperature were also shown to vary with gas preheat temperature [2, 17, 18]. Other parameters expected to affect the cold spray deposition process include the powder size [6, 19], particle position in the gas jet [20] and particle impact angle [18].

The present study is based largely on the experimental testing of splat adhesion strength, exploring the effect of deposition conditions such as velocity, gas preheat temperature and substrate temperature on the deformation behaviour and splat adhesion strength of Ti and Ti6Al4V splats deposited onto Ti and Ti6Al4V substrates. Helium and nitrogen gases were used to obtain a range of particles velocities at varied gas temperatures. The effect of the particle velocity and gas temperature was explored through measurement of the particle deformation and particle adhesion strength. The adhesion strength of individual cold spray splats was deposited on substrates at ambient and elevated temperatures and tested with a micromechanical test technique that measures the splat adhesion strength, as first reported in publication by R.R. Chromik et al. [8], where the technique was termed a "modified ball bond shear test". Here the same technique is used, where the adhesion strength of the splats was measured from the shearing forces exerted by the splat on the wedge shape tip [8]. Adhesion testing was performed on varied splat sizes and on splats at varied position across the single deposition pass in order to test the effect of the particle size and the particle position in the gas jet on the splat deposition. Light optical microscopy (LOM) and scanning electron microscopy were used for evaluation of splat deformation mechanisms and characterization of the splat substrate bonding interface. Three splat shearing regimes were identified by observation of residual shear tracks on the substrate surface and the features in the force-displacement curves recorded during tests.

2. Experimental Procedure

2.1: Cold spray deposition

Cold sprayed splats were prepared as Ti and Ti6Al4V deposited onto substrates of the same material, where the substrate was either heated or left at ambient conditions. Cold spray splats were obtained by powder acceleration with a Kinetic 4000 cold spray gun through MOC24 nozzle (CGT GmbH, Germany). In order to obtain individual particle deposition, the powder feeding rate of 1 - 2 g/min and gun traveling speed of 1 m/min were used.

The powder consisted of commercially pure – cp Ti powder and Ti6Al4V powder with 0 - 45 μm particle size and 29 μm average particle diameter provided by Raymore Inc. (Boisbriand, QC, Canada). The powder size distribution and average particle diameter were measured and published previously [21]. The splats were deposited on as-received and on preheated Ti or Ti6Al4V annealed substrates with 3 mm plate thickness (McMaster-Carr, Aurora, OH, USA). The substrates were degreased with acetone prior to the cold spray splat deposition but were otherwise left in the as received surface state, which was a milled finish. Some substrates were also preheated to 400°C with three heating elements mounted in the sample holder. A thermocouple was placed inside the sample holder and a temperature of 400°C was maintained through the cold spray deposition of splats.

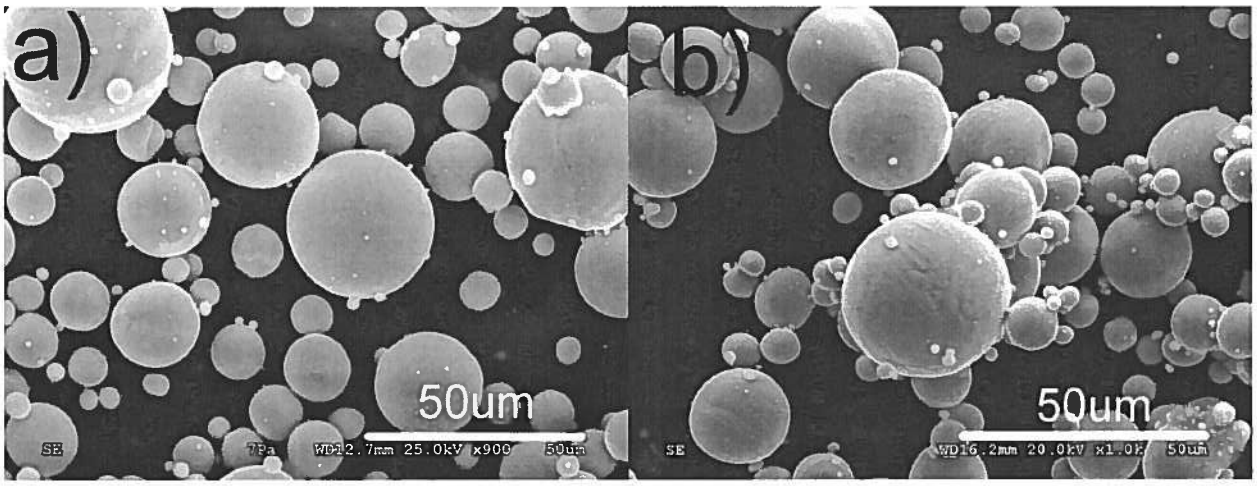

Figure 2: Micrographs obtained by SEM for the a) Ti Powder and b) Ti6Al4V Powder.

The particle velocity was measured, in a free jet, with a DPV2000 (Tecnar Automation, St. Bruno, QC, Canada). Velocities ranging from 580 to 1140 m/s were obtained by preheating and pressurizing nitrogen or helium gas from 25°C to 800°C and from 1 MPa to 4 MPa. An average velocity of 1000 – 2000 particles was taken for each deposition condition. For the deposition conditions with nitrogen gas, the velocity measurements were carried at 4 cm distance from the gun nozzle. For the deposition conditions with helium gas, the distance from the nozzle was maintained at 8 cm. The same gun nozzle-substrate distance was used during cold spray splat deposition.

2.2: Microstructural Characterization

The cold sprayed samples were cut in cross-section and mounted into the cold mount epoxy. The samples were then polished according to a standard polishing procedure for Ti [22] with a final step of 0.05μm colloidal silica with 10% hydrogen peroxide. The samples were then etched with Kroll's reagent consisting of 3% HNO_3, 2% HF and distilled water.

The etched images of splats were examined with light optical microscope (LOM) and a variable pressure scanning electron microscope (Hitachi S-3000N VP-SEM, Japan). LOM was used to measure the height and width of the cold spray splats with image analysis software (Clemex Vision Professional 5.0, Clemex Technology Inc., Longueuil, QC, Canada). Splat width - w, to height - h, ratio was then used to calculate the splat flattening ratio. Flattening ratio is a measure of degree of splat deformation and is described in Eq. 1 [4, 7, 12]. Typically, a flattening ratio of 10 - 30 splats was calculated and an average value was taken for each deposition condition. In case of very low deposition velocity conditions (below 650 m/s), the deposition efficiency of splats was very low and for that reason the average of 3 or more splats was taken. The standard deviation on the mean was used as the error bar.

$$FR = \frac{w\,(\mu m)}{h\,(\mu m)} \qquad \text{Eq.1}$$

2.3: Mechanical Property and Surface Characterization of Starting Materials

The hardness of the Ti and Ti6Al4V feed-stock powder and Ti and Ti6Al4V substrates was measured by nanoindentation with two systems, either Ubi 3 or Triboindenter (Hysitron Incorporated, Minneapolis, MN). The hardness and reduced elastic modulus were measured with a Berkovich tip at 1 mN load with 200 μN/s loading/unloading rate and 1 second holding time. Data was analyzed using the Oliver and Pharr method [23]. Average property values were taken from over 40 data points.

The surface roughness of the substrates was determined with contact profilometer (Veeco Instruments, CA, USA). The average surface roughness (Ra) was determined from 6 lines cans of 1 cm in length on Ti and Ti6Al4V substrate. The scans were carried along and across the substrate length. Average surface roughness was taken from the six measurements.

2.4: Splat Adhesion Testing

Shear testing was performed using a Micro-Combi Scratch Tester (CSM Instruments, Inc., Needham, MA, USA) with a wedge shaped indenter [8]. The adhesion strength of splats was measured by applying a normal force, F_N of 30 or 300 mN onto the wedge shaped tip (100 μm in width) that was placed a distance of approximately 29 μm, away from the splat. The substrate was then moved at 150 μm/min rate below the tip, as can be seen in Figure 3.

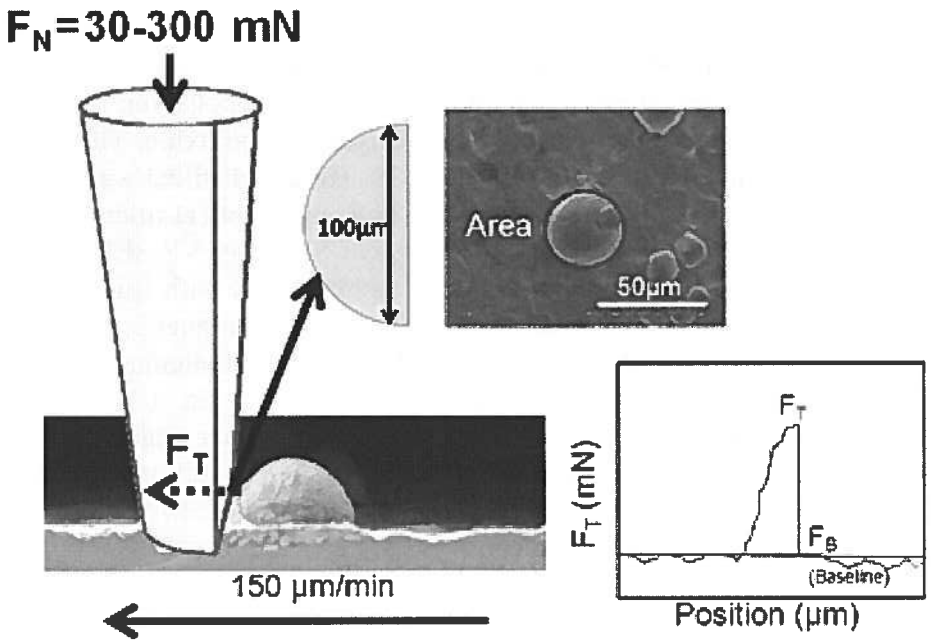

Figure 3: A schematic diagrams of splat adhesion testing. On the left, a cross-sectional view and, on the upper-right, a top-down view of the test are provided. In the upper right, the cross-section area of the splat is noted, which is used in the calculation of the splat adhesion strength. In the lower-right, an example of the force-displacement curve obtained during the shearing of a splat.

The adhesion strength of the splat was calculated as a function of tangential force, F_T, exerted on the tip, the baseline force F_B and the splat area, according to Eq.2. The splat area A, was measured prior to splat shearing according to equation 3 where w is splat diameter measured with an optical microscope mounted on the Micro-Combi Scratch Tester.

$$Adhesion\ Strength\ (MPa) = \frac{F_T - F_B}{A} \qquad \text{Eq.2}$$

$$Area = \pi\left(\frac{w}{2}\right)^2 \qquad \text{Eq.3}$$

The shearing was performed on 5 - 10 splats with 35 - 50 µm in diameter. This range of splat diameters was selected and used splat of for every deposition conditions in order to maintain the same range of the pre-impact particle diameters centered about the average particle size of 29 µm. The particle pre-impact diameter was calculated by assuming that upon the impact the splats deforms from a spherical geometry into oblate spheroid geometry according to Eq.4.

$$d\ (\mu m) = (w^2 h)^{1/3} \qquad \text{Eq.4}$$

The splat width, *w*, and splat height, *h*, were measured with a light optical microscope on the Micro-Combi Scratch Tester. The splat height was measured by taking the difference between

the focusing distance of the upper splat crown and the focusing distance of the substrate material. The error on the measurement was between 1 and 10 %.

3 – Results

3.1 – Mechanical Property Characterization

In Table 1 the hardness and reduced elastic modulus of the feed-stock Ti and Ti6Al4V powder as well as Ti and Ti6Al4V substrates are summarized. The hardness of the commercially pure Ti powder and Ti substrates were identical at 3.1 GPa with reduced modulus of the material very close to the theoretical modulus of Ti at 116 GPa. The hardness of the Ti6Al4V powder and substrate was higher than that of the pure Ti materials. This is to be expected from an alloyed material. The hardness of the Ti6Al4V powder was 4.8 GPa while the hardness of the substrate was 5.8 GPa. The reduced modulus of the Ti6Al4V materials was also slightly higher than that of the pure Ti materials. The difference in the hardness and reduced modulus measurements can be explained by the differences in composition and the manufacturing processes involved in the casting of the substrate and gas atomization of the powder.

Also in Table 1, the average surface roughness of as received Ti and Ti6Al4V substrates is also listed. Both substrates demonstrate comparable Ra values that fall within the standard deviation on each measurement.

Table 1: Properties of Ti and Ti6Al4V powder and substrates

Material	Hardness (GPa)	Reduced Elastic Modulus (GPa)	Surface Roughness Ra (μm)
Ti powder	3.1 ± 0.4	114 ±10	-
Ti substrate	3.1 ± 0.3	125 ± 6	0.60 ± 0.12
Ti6Al4V powder	4.8 ± 0.3	104 ± 5	-
Ti6Al4V substrate	5.8 ± 1.1	123 ± 11	0.52 ± 0.14

3.2 – The effect of the gas temperature and pressure on the deposition velocity

Ti or Ti6Al4V powder was deposited onto Ti or Ti6Al4V substrate at supersonic velocities ranging from 580 to 1140 m/s. A wide range of velocities was obtained by varying the nitrogen or helium gas temperature from 25°C to 800°C and by changing the gas inlet pressure from 1 – 4 MPa. The average deposition velocity increased with increase in the gas temperature but also increased with increase in the inlet gas pressure. The nature of the gas also affected the deposition velocity of the particles. At similar gas preheat temperature and pressure, higher velocities were obtained with helium gas when compared to nitrogen gas. The deposition conditions and the corresponding average deposition velocities are listed in Table 2.

Table 2: Splat Deposition Conditions

Gas	Ti Powder on Ti (at RT and at 400°C)			Ti6Al4V Powder on Ti6Al4V (at RT and at 400°C)		
	Gas Temperature (°C)	Gas Pressure (MPa)	Deposition Velocity (m/s)	Gas Temperature (°C)	Gas Pressure (MPa)	Deposition Velocity (m/s)
Nitrogen	300	2	580	300	2	590
	300	3	625	300	3	631
	300	4	642	300	4	657
	500	2	636	500	2	646
	500	3	694	500	3	701
	500	4	724	500	4	741
	750	3	770	750	3	778
	800	4	825-852*	800	4	834
Helium	Ti on Ti (at RT)			Ti6Al4V on Ti6Al4V (at RT)		
	Gas Temperature (°C)	Gas Pressure (MPa)	Deposition Velocity (m/s)	Gas Temperature (°C)	Gas Pressure (MPa)	Deposition Velocity (m/s)
	50	1	616	25	1	562
	50	2	787	25	2	787
	50	3	877	-	-	-
	350	2	877	350	2	964
	350	3	950	350	3	1052
	350	4	1140	350	4	1115

**Particle velocity measured at a different time frame*

In Table 2 some of the samples were produced at different time frame (one year later) and the deposition velocity for a given gas preheats temperature and pressure condition was re-measured prior to sample preparation. The measurements made at a later time frame are indicated by a star. The difference in the particle velocities can be attributed to the changes made in the cold spray system over time including the replacement of the gun nozzle. Some of the particle velocity measurements, listed in the Table 1, were previously published [8, 24].

While the gas temperature and pressure are the main parameters affecting particle velocity, other parameters such as the particle position in the gas jet [20] and the size of the powder particles [6] can also have an effect on the particle velocity. The particles located at the edge of the jet travel at a lower speed when compared to particles traveling at the center of the jet [20]. At the same time, smaller particles travel at a faster speed than larger particles [6]. Due to these facts, the actual velocity for each deposition condition follows a Gaussian distribution as shown in Figure 4.

In Figure 4, three particle velocity distributions for low, intermediate and high deposition velocity conditions are shown. At low deposition conditions, most of the particles travel at an average particle velocity of 625 m/s however a small portion of particles reach the minimum critical deposition velocity for Ti at 700 m/s. Similarly, at high deposition condition where most of the particles travel at average deposition velocity of 770 m/s some of the particles travel below the minimum critical velocity.

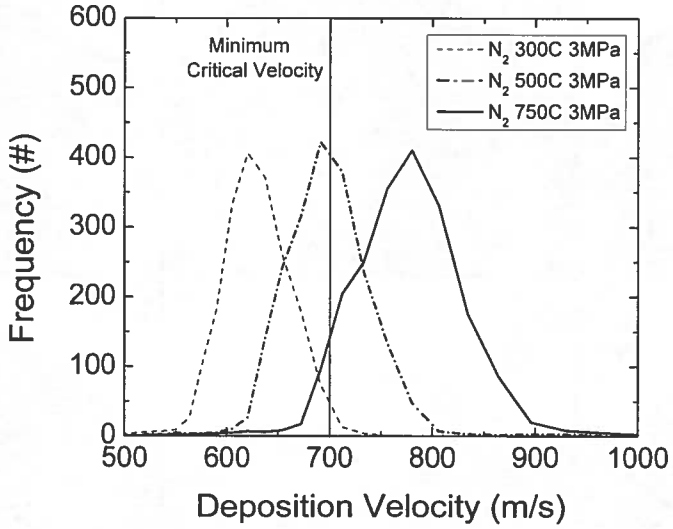

Figure 4: Particle velocity distribution for low, intermediate and high deposition conditions of Ti powder accelerated with nitrogen gas. The minimum critical velocity for Ti is indicated by vertical intercept at 700 m/s and according to Schmidt et al.[6]

To circumvent some of the uncertainty in the particle velocity measurements, mainly the particles at the center of the deposition pass were examined. This position corresponds to those particles near the center of the gas jet, where the velocity is the highest. Furthermore, measurements were carried out on particles close to the average feed-stock powder diameter of 29 μm, removing some of the variation in velocity associated with particle size. Additionally, these particles are the most populous within the velocity distributions, such as those in Figure 4. Thus, it is expected that particles tested in this manner arrived at the average velocity for the given spray condition or higher. Other testing was carried out as a function of position across the gas jet or as a function of particle size along the deposition pass. In these cases the variation in properties measured is a function of velocity, due to its variation across the gas jet and with particle size.

3.3 – Effect of particle velocity and as preheat temperature on splat deposition

In Figure 5, representative SEM images of the etched Ti a)-c) and Ti6Al4V d-f) splats deposited at increasing deposition velocities on Ti and Ti6Al4V substrates are shown. Ti splats deposited on Ti substrate as well as Ti6Al4V splats deposited on Ti6A4lV substrate showed three different deposition regimes. As can be seen in Figure 5a and 5d, at deposition velocity approaching the critical velocity (~700m/s) the splat deformation was not extensive and material jetting region was limited. Bonding took place mainly through conformal adhesion between the splat and the substrate. As the deposition velocity increased, the splats became more deformed and extensive material jetting took place, as can be seen in Figure 5b and 5e. Regions of continues bonding are observed in the splat at 45 degree angle from the splat impact site.

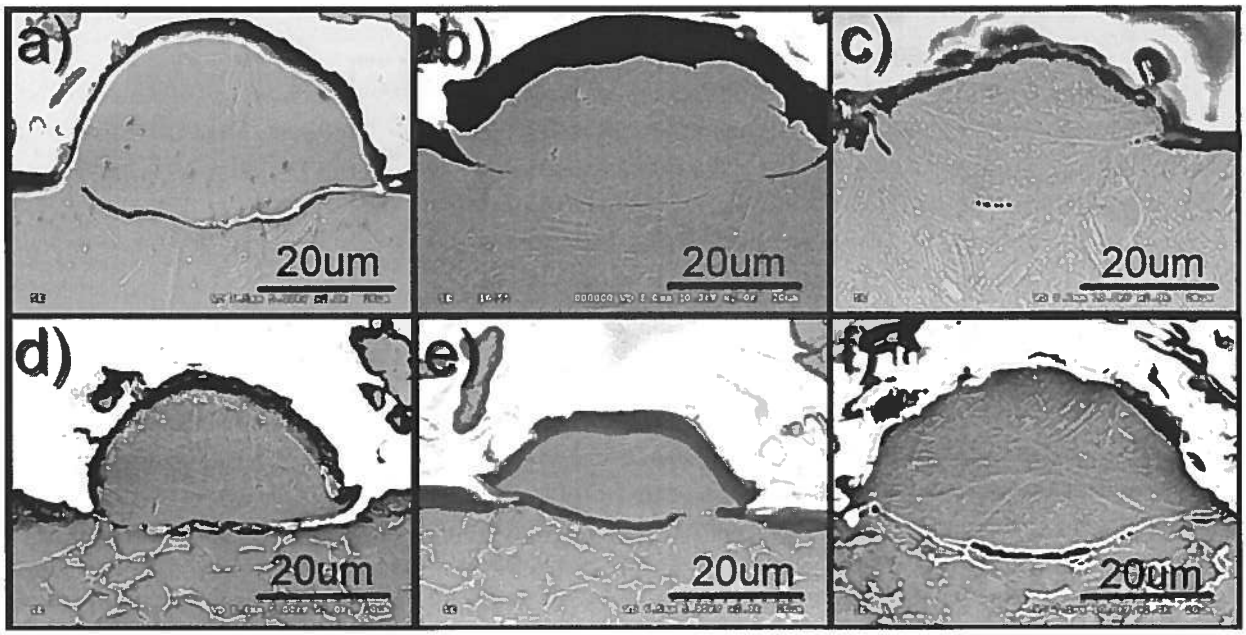

Figure 5: Etched SEM cross-sectional micrographs of Ti splats deposited on Ti at a) 724m/s (N_2 at 500°C 4MPa) b) 825m/s (N_2 at 800°C 4MPa) c) 1173m/s (He at 350°C 4MPa) and Ti6Al4V splats deposited on Ti6Al4V substrate at d) 741m/s (N_2 at 500°C 4MPa) e) 834m/s (N_2 at 800°C 4MPa) f) 1115m/s (He at 350°C 4MPa).

As the deposition velocity increased even further, the substrate deformation became more pronounced. Figure 5c demonstrates this behaviour. In Figure 5c, the substrate deformation contributed to the formation of a very intimate, possibly metallurgical, contact between the Ti splat and substrate. Under same depositions, Ti6A4lV splats deposited on Ti6Al4V showed a lower degree of substrate deformation and bonding when compared to Ti splats deposited on Ti substrate (see Figure 5e). The bonding interface between Ti6Al4V splat and substrate was not continuous and the etched cross-section revealed the presence of the splat/substrate junction as seen by a bright feature at the interface (see Figure 5f).

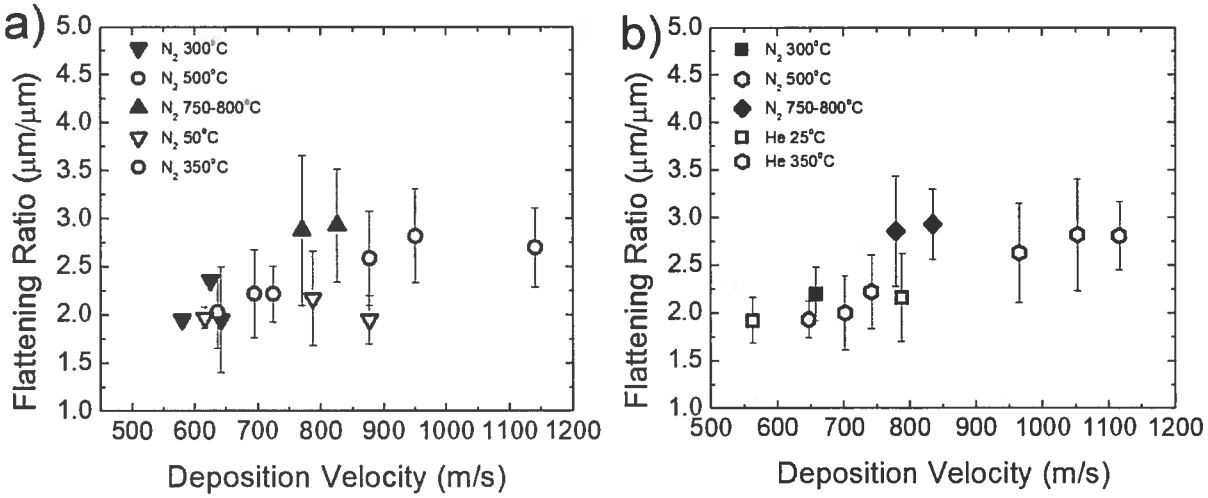

Figure 6: Flattening ratio versus deposition velocity for a) Ti splats and b) Ti6Al4V splats deposited with nitrogen and helium gases at varied gas preheat temperatures.

The extent of splat deformation was measured in terms of Eq. 1 from the etched images of splats similar to the ones shown in Figure 5 and was plotted as a function of particle deposition velocity (see Figure 6). As can be seen in Figure 6a, Ti splat flattening ratio, increased with increase in the deposition velocity up to 850 m/s but then stabilized if not decreased at 1173 m/s. These measurements were consistent with the observations made from Figures 5a-c. The splat deposited at 825 m/s was more deformed than the splat deposited at 724 m/s however the splat deposited at 1173 m/s had a lower width to height ratio due to substrate deformation. Average Ti substrate deformation depth was calculated from SEM images of 10 - 30 etched splat cross-sections and was measured to be 2.1 ± 2.2 μm at 825 m/s and 8.1 ± 4.3 μm at 1140 m/s which is approximately 10% and 40% of the splat height.

The flattening ratio of Ti6Al4V splats deposited on Ti6Al4V, shown in Figure 6b, increased from roughly 2 at 650 m/s to 3 at deposition velocity of 850 m/s. No splats were deposited below 650 m/s and were not analysed. The splat flattening ratio did not increase at higher deposition velocities obtained with helium gas. The cross-sectional SEM image of the splat deposited at 1115 m/s and shown in Figure 5f had a very limited substrate deformation when compared to Ti substrate seen in Figure 5c. T6Al4V substrate deformation depth increased from 0.5 ± 1.3 μm at 834 m/s (which is the roughness of the substrate) to 4.6 ± 1.6 μm at 1115 m/s.

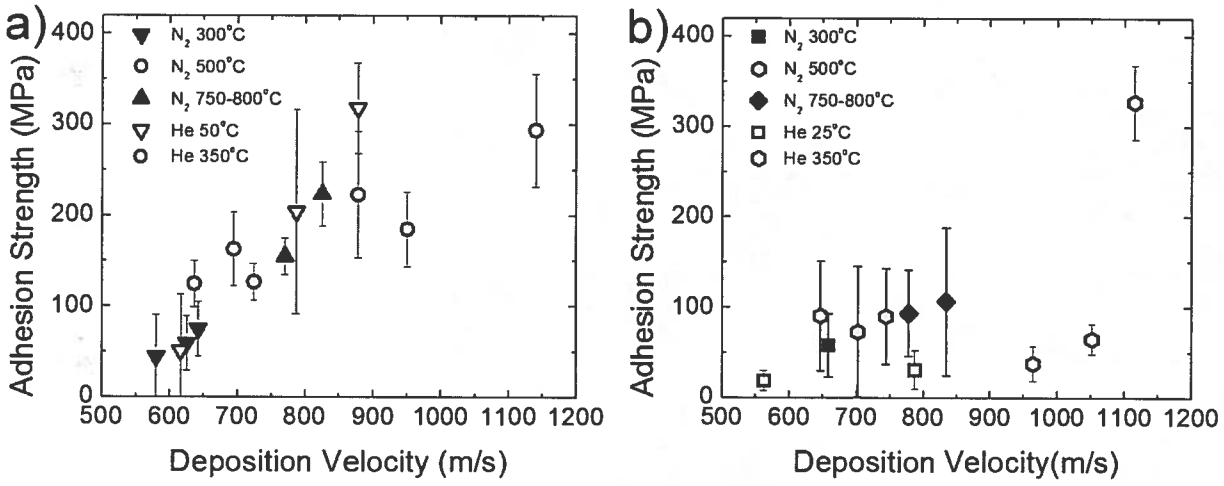

Figure 7: Adhesion strength versus deposition velocity for a) Ti splats deposited on Ti substrate and b) Ti6Al4V splats deposited on Ti6Al4V substrate with nitrogen and helium gases at varied gas preheat temperatures.

In Figure 7, a steady increase in the splat adhesion strength was measured with increase in the deposition velocity unlike the splat flattening ratio. For Ti splats deposited on Ti substrate at velocities greater than 800 m/s, the splat adhesion strength approaches the theoretical shear strength of Ti at 380MPa [25]. The results correlate well with the SEM image shown in Figure 5 that showed an almost continuously bonded splat/substrate interface.

The adhesion strength of Ti6Al4V splats deposited on Ti6Al4V substrate was lower than that of Ti splats deposited on Ti substrate and was significantly lower than the shear strength of Ti6Al4V at 550MPa [25]. The adhesion strength in the Ti6Al4V splats was mostly constant at 100MPa and only reached ~320MPa at a the highest deposition velocity of 1115m/s. Ti6Al4V

has higher shear strength when compared to pure Ti and higher impact velocities are required to induce adiabatic shear.

It is interesting to note that at same deposition velocities, Ti and Ti6Al4V splats deposited with at higher gas preheat temperature demonstrated a slightly higher flattening ratio. Furthermore, at deposition velocities below the critical velocity range, splats deposited with a gas at higher gas preheat temperature but same deposition velocity also showed better adhesion strength..

3.4 – Splat shearing behaviours

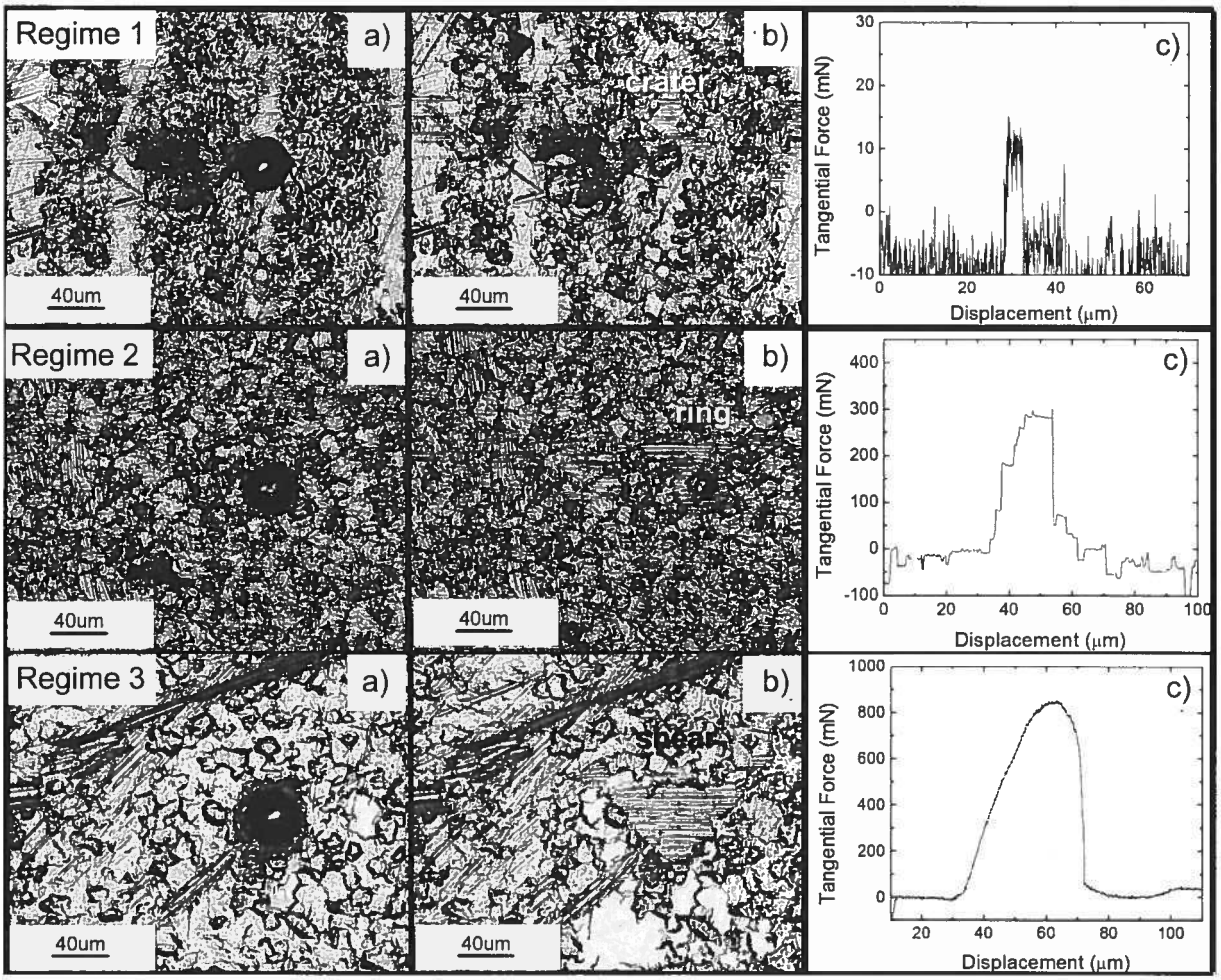

Figure 8: Three regimes of splat shearing behavior are shown with corresponding top view LOM images of splats a) before shearing and b) after shearing, c) with respective tangential force vs. displacement curves.

During the adhesion testing, three types of splat shearing regimes were observed and are shown in Figure 8. In the first shearing regime, a rapid and a bit jumpy increase in the tangential forces with respect to the stylus displacement was observed and was followed by a rapid drop in the tangential forces. The total stylus displacement associated with the shearing event was minimal. Also, the very small rise in the tangential forces, 12 mN, with tip displacement indicates a poor material resistance to deformation and therefore poor splat adhesion strength.

The first shearing regime was typically observed for splats deposited below the critical velocity (700 m/s for Ti). In second shearing regime, a smooth rise in the tangential forces was measured with stylus displacement into the splat. As opposed to the first shearing regime, the peak tangential force reached 300 mN and was followed by a drastic drop in tangential forces half way (~20 μm) into the splat. Splats demonstrating this behavior also have higher adhesion strength compared to those of regime 1. Upon close examination of the sheared region, the shear tracks on the substrate form a ring around the impact crater. The ring formation had the outline of the sheared splat. Finally, the third shearing regime was defined by a homogeneous rise and drop in the tangential forces during the shearing of the splat. As compared to regimes 1 or 2, regime 3 had no drastic drop in the tangential forces at the end of the shearing event and the width of the tangential force peak was roughly the width of the sheared splat. For the third shearing regime, the shear tracks formed a full circle with no crater formation. The splats demonstrating this type of shearing behaviour had adhesion strength approaching the theoretical shear strength. The third shearing regime was observed for Ti splats deposited at 1100 m/s. Ti6Al4V splats deposited on Ti6Al4V substrate only exhibited regimes 1 or 2 and never demonstrated the behaviour of regime 3.

In Figure 9, SEM images of the Regime 2 sheared region with ring formation around the impact crater are shown. The impact crater demonstrated a region with dimples mainly observed at the rim inside the crater wall. The dimples are indicative of a ductile fracture of a Ti [26, 27] and therefore indicate that a metallurgical bonding in that region. Regime 2 shearing behavior was typically observed for splats deposited above 800 m/s. It is interesting to note that the center of the crater has a smooth, dimple-free surface which indicates that no bonding took place in that region. The observations of where bonding took place correlated well with the SEM images of the splat cross-sections shown in Figure 5b and e.

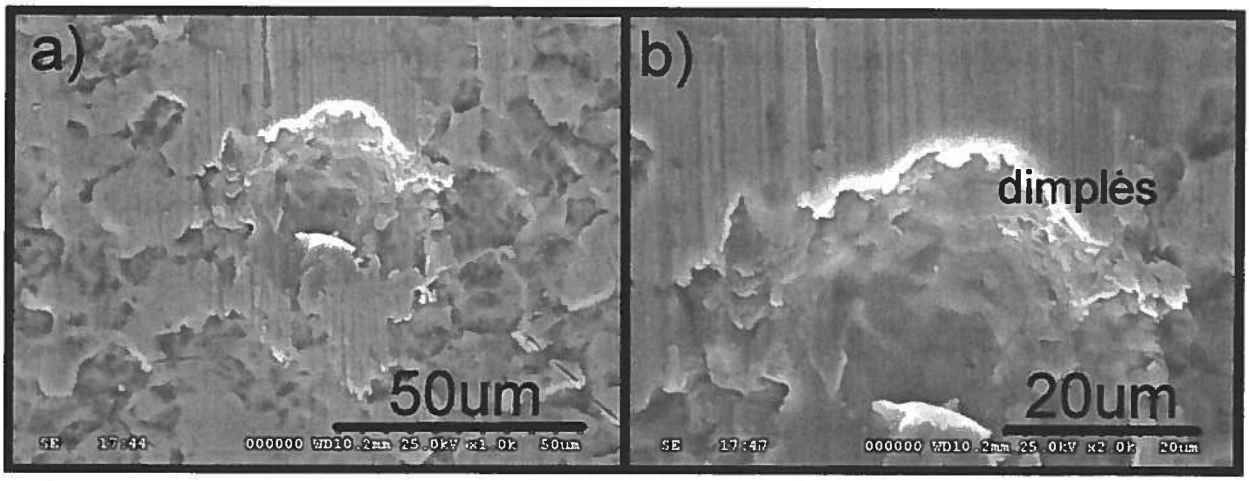

Figure 9: SEM image of the regime 2 sheared region at low a) and at high b) magnification. The shear band rings surrounding the crater are shown with dimpled ductile fracture at the inside rim of the crater.

Based on the force displacement curves, Ti and Ti6Al4V splats, sheared from Ti and Ti6Al4V substrates, were classified into one of the shearing regimes illustrated in Figure 8. A value of 1 was assigned to splats shearing according to regime 1, 2 for regime 2 and 3 for regime 3. However, a small number of splats exhibited behaviour "in-between" the three regimes identified in Figure 8. For those in-between regimes 1 and 2, a value of 1.5 was assigned. These

splats sheared with the peak tangential force occurring before the displacement reached half of the splat width, but did demonstrate a peak shape more similar to regime 2 than regime 1. For splats in-between regimes 2 and 3, the value of 2.5 was assigned. These splats had a peak in the shearing force at a displacement greater than the half splat width but demonstrated the rapid drop in load at the end of the test that was typical of regime 2. All tested splats (5 to 10 splats in total) were analysed for each condition and an average shearing regime was plotted as a function of deposition velocity, as shown in Figure 10.

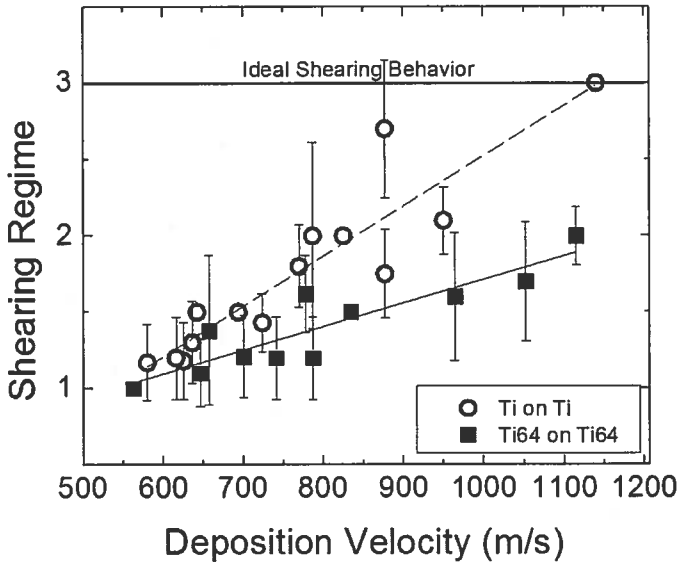

Figure 10: Shearing regime as a function of depositions velocity for Ti and Ti6Al4V splats on Ti and Ti6Al4V substrates.

In Figure 10, the splat shearing regime had a linear relationship with the deposition velocity. As the deposition velocity increased, the splat shearing behavior approached the ideal, regime 3 shearing behavior with near theoretical adhesion strength of the cold sprayed material. Ti splats deposited on Ti substrate reached regime 3 at 1140 m/s. While an ideal shearing behavior was observed, the adhesion strength of the splats deposited at this velocity was measured to be below the theoretical 360 MPa and at 300 MPa.

The cross-sectional images of the splat deposited at this velocity is shown in Figure 5c and indicated that not all of jetting region participated in the splat bonding. Thus, the actual splat contact area calculated according to Eq. 3 was slightly overestimated and may explain why an apparently fully bonded splat does not have strength closer to the expected value. As opposed to Ti, Ti6Al4V splats deposited on Ti6Al4V substrate never exhibit the 3rd shearing regime. The linear fit to the data in Figure 10 indicated that Ti6Al4V splats deposited on Ti6Al4V substrate would reach 3rd shearing regime at 1829 m/s. Such velocity is unrealistic in terms of the present cold spray system capabilities [28] and furthermore does not take into account the onset of erosion expected at extreme deposition velocities [6].

3.5 Effect of powder particle size and position in the gas jet.

In the previous sections, the adhesion strength was measured for splats with similar pre-impact particle diameter of ~ 29 μm as calculated according to Eq 4. In industrial applications, powder size distribution will vary and a better understanding of the effect of the particle size on the adhesion strength of splats is required. In Figure 11, the effect of the particle size on the splat adhesion strength was evaluated. As can be seen in Figure 11, the adhesion strength of the smaller splats was higher when compared to larger splats. The splats with particles size between 10 and 20 μm had adhesion strength in the range of 250 to 300 MPa while 40 to 60 μm splats have particle adhesion strength ranging between 150 and 250 MPa. The results correlated well with the general understanding of particle flight dynamics where particles of smaller size were shown to have a higher in flight velocity when compared to particles of larger size [2, 29] and consequently a better adhesion strength.

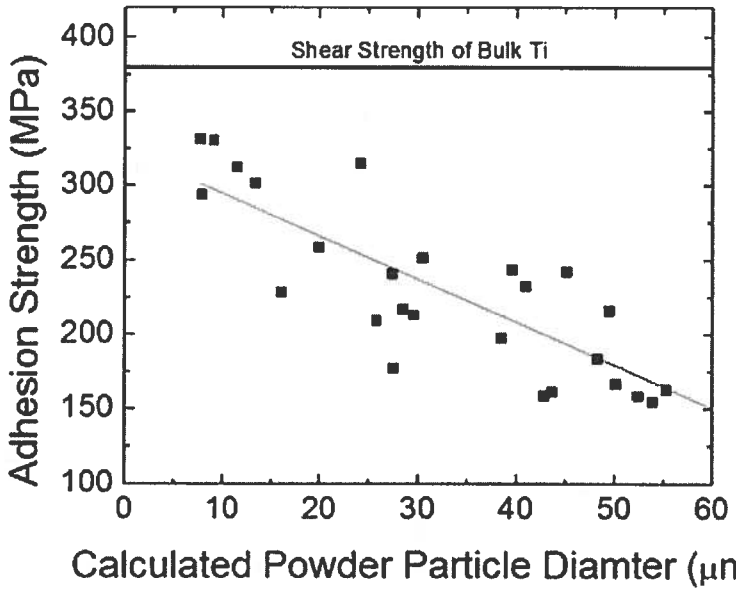

Figure 11: The adhesion strength of Ti splats deposited at 852m/s (N_2 800°C and 4MPa) with respect to the particle size calculated according to Eq.4. Splat adhesion was measured at the center of the deposition track. A decrease in the particle adhesion strength was observed with increase in the particle size.

The powder particle position in the gas jet can have an effect on the particle velocity. A particle in the center of the gas jet travels at a higher velocity than splats at the edges of the jet [20]. The particle deformation and bonding strength can be therefore affected. In Figure 12, the splat adhesion strength was measured across the width of a deposition pass (i.e. perpendicular to the gun traverse direction). The adhesion strength of splats with roughly same particle diameter (~ 29 μm) was measured. The splat adhesion strength was highest (~250 MPa) in the 4 - 8 mm which corresponded to the center of the pass width. The lowest adhesion strength, ranging from 0 - 100 MPa, was measured for the splats located at the edge of the pass at 0-4 and 8-12 mm.

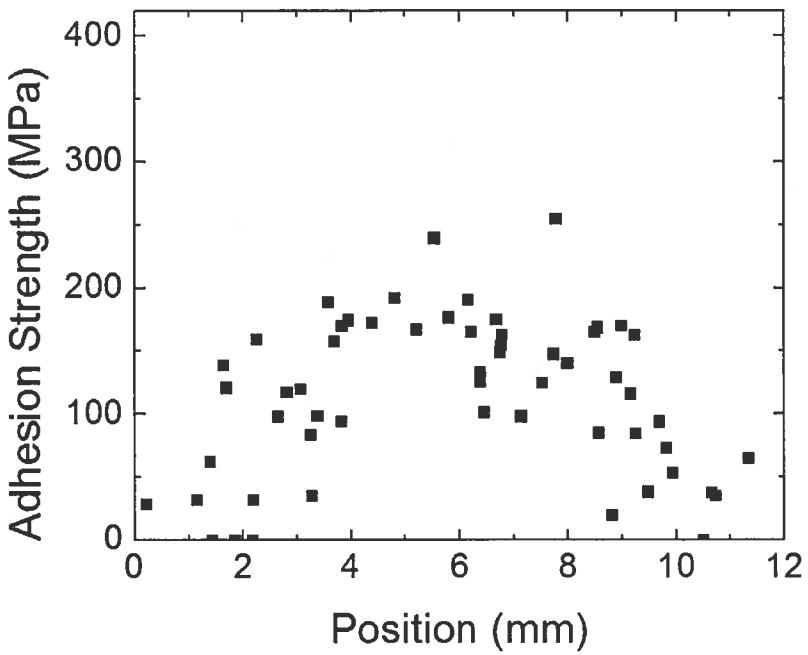

Figure 12: Adhesion strength of Ti splats as function of their position across the deposition pass. These splats were deposited at 800°C 4MPa gas conditions and splats tested had a ~29 μm particle pre-impact diameter. Lower adhesion strength is measured for splats deposited at the edge of the pass.

3.6 - Substrate temperature effect

The splats examined in the present work were deposited as a single pass on the substrate at room temperature. Previous studies have shown that the temperature of the substrate material increases with the successive splat impact events and the warm air from the gas jet [30]. As a result of splat impact with the substrate and adiabatic shear, the temperature of the substrate will rise [1, 11, 17, 30] and could realistically reach 400°C. In order to "simulate" the temperature rise of the gas jet and successive impacts, substrates were preheated to 400°C prior to splat deposition. Measurements of the splat adhesion strength from these splats may mimic more closely the bonding that takes place in a full coating.

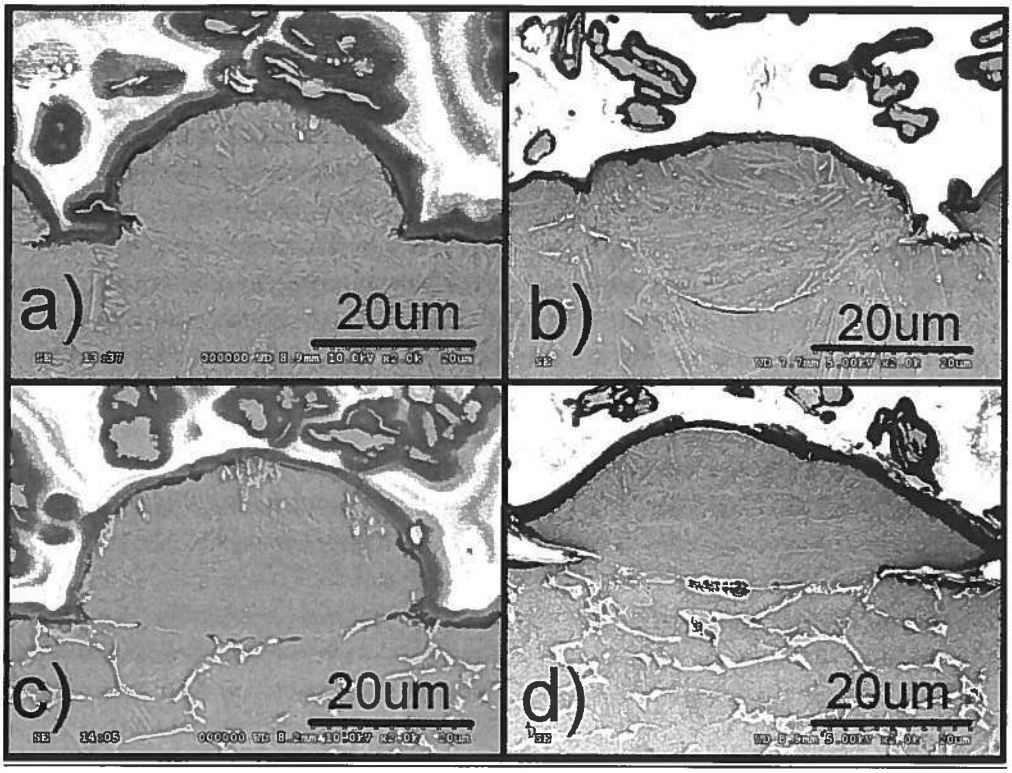

Figure 13: Etched cross-sectional micrographs obtained with SEM for a) Ti splats deposited at 724m/s (N_2 at 500°C 4MPa) on Ti substrate preheated to 400°C, b) Ti splats deposited at 825m/s (N_2 at 800°C 4MPa) on Ti substrate preheated to 400°C, c) Ti6Al4V splat deposited at 741 m/s (N_2 at 500°C 4 MPa) on Ti6Al4V substrate preheated to 400°C and d) Ti6Al4V substrate deposited at 832 m/s (N_2 at 800°C 4 MPa) on Ti6Al4V substrate preheated to 400°C.

As can be seen in Figure 13a and b, Ti splats deposited on preheated Ti substrate showed a more extensive, bonded interface when compared to Ti splats deposited on Ti substrate at ambient temperature under same deposition conditions, as shown in Figure 5a and 5b. Furthermore, Ti splats deposited at 805 m/s (see Figure 13b) showed similar substrate deformation and bonding as one obtained at much higher deposition velocity with ambient substrate conditions (see Figure 5c). The average depth of the preheated Ti substrate deformation was measured to be 4.2 ± 2.8 μm and was higher than for the non-preheated substrate at 2.1 ± 2.2 μm measured for 825 m/s deposition condition. For Ti6Al4V splats deposition on preheated Ti6Al4V substrate and shown in Figures 13c and 13d, no significant substrate deformation even after substrate preheating was observed. The Ti6Al4V preheated substrate deformation depth was measured to be 0.8 ± 1.3 μm and was very similar to the deformation depth of the non-preheated substrate at 0.5 ± 1.3 μm at 834 m/s deposition condition.

Flattening ratio for Ti and Ti6Al4V splats deposited on preheated substrates is shown in Figure 14. The splat flattening ratio measurements for Ti splats on preheated Ti substrate demonstrated a slight decrease when compared to the same splats deposited on unheated substrates. This behavior can be once again explained by substrate deformation observed in Figure 13b. On the other hand, the flattening ratio of Ti6Al4V splats deposited on preheated substrates was similar to that of Ti6Al4V splats on unheated substrates as shown in Figure 14c.

The results correlate well with the SEM images shown in Figure 13 where no substrate deformation was observed.

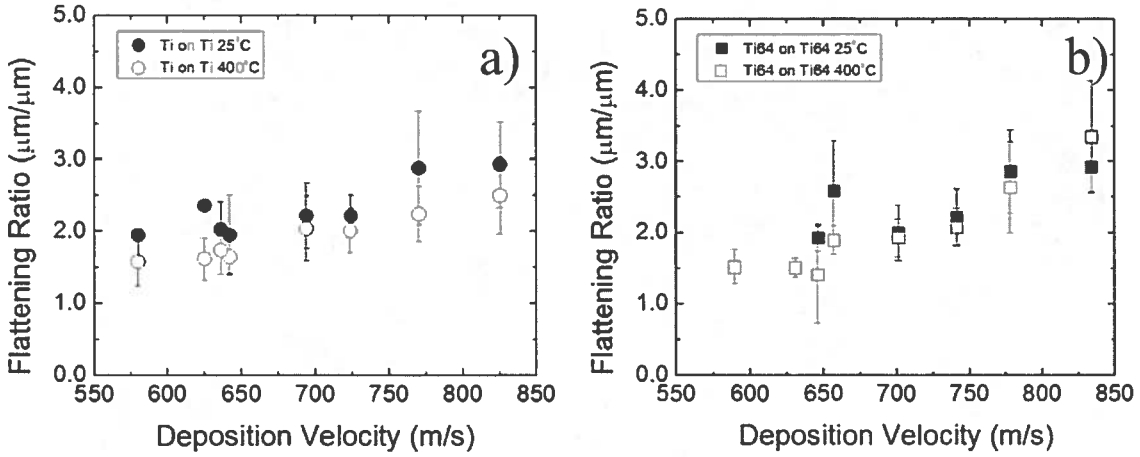

Figure 14: Flattening ratio of a) Ti splats deposited on Ti substrate at 25°C and preheated to 400°C and b) Ti6Al4V splats deposited on Ti6Al4 substrate at 25°C and preheated to 400°C. The flattening ratio decreases for Ti splats deposited on preheated substrate. No change in the flattening ratio was measured for Ti64 splats deposited on Ti64 substrate at 25°C or at 400°C.

Unlike the similarity for flattening ratios from preheated and unheated substrates, a dramatic increase in the splat adhesion strength was measured for Ti and Ti6Al4V splats deposited on preheated substrates. In Figure 15a, the adhesion strength of Ti splats reached a mark of ~220 MPa at deposition velocity of 650 m/s, a significant improvement from 100 - 120 MPa measured for the same velocity splats on unheated substrates. A similar increase in the adhesion strength was measured Ti6Al4V splats deposited at slightly higher deposition velocity of 700 m/s in Figure 15b.

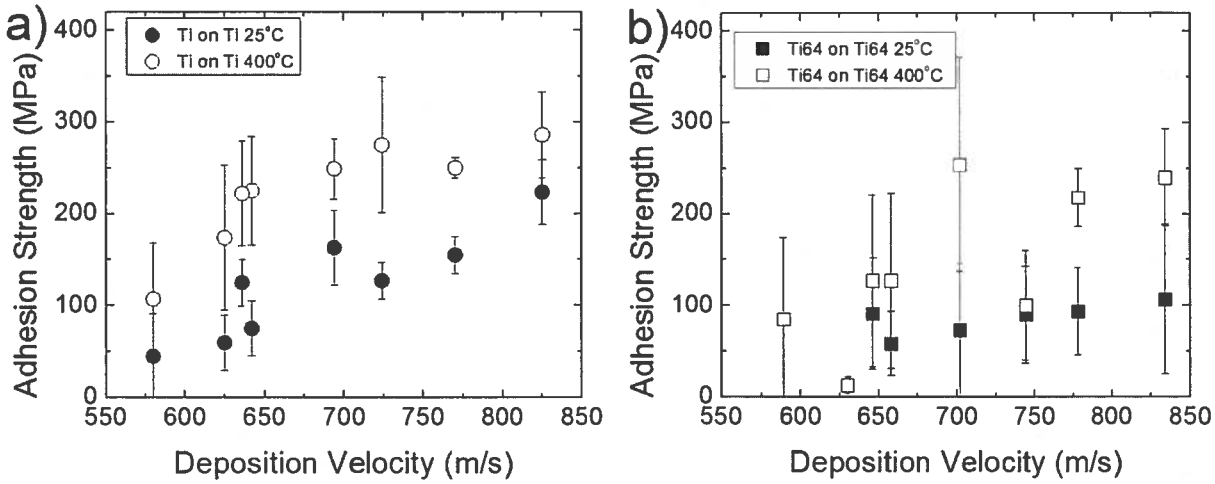

Figure 15: Splat adhesion strength as a function of deposition velocity for a) Ti splats deposited on Ti substrate at 25°C and preheated to 400°C b) Ti6Al4V splats deposited on Ti6Al4 substrate at 25°C and preheated to 400°C. The adhesion strength is higher for splats deposited on preheated substrate.

In Figure 16, a plot of the average shearing regime versus deposition velocity showed that for Ti splats deposited on preheated substrates, the ideal regime 3 behavior was reached at 825 m/s. For non-preheated substrates, this occurred at a much higher velocity of 1100 m/s. For Ti6Al4V splats, they only the average shearing regime reached a value of 2 at 834 m/s as can be seen in Figure 16. There was still an improvement for Ti6Al4V with substrate heating, as for these conditions the regime 3 behaviour was reached at 1220 m/s, compared to the unrealistic 1800 m/s observed for non-preheated conditions

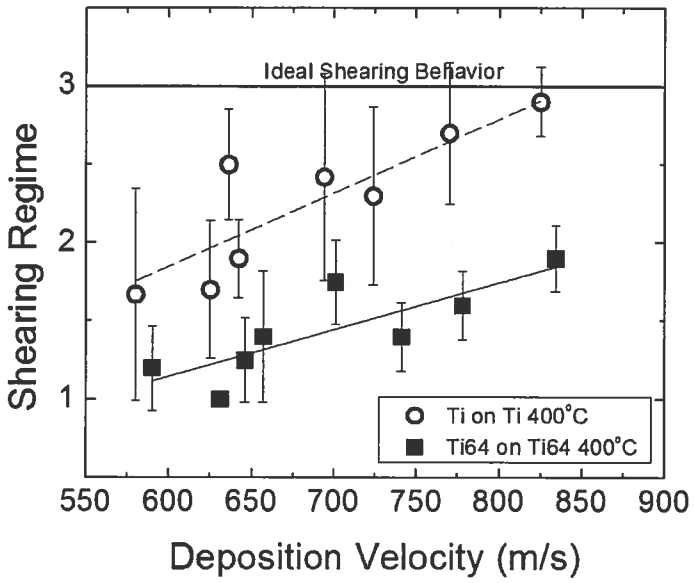

Figure 16: Average shearing regimes as a function of deposition velocity for Ti and Ti6Al4V splats deposited on preheated Ti and Ti6Al4V substrates.

4. Discussion

The most widely accepted mechanism for metallurgical bonding in cold sprayed metals is the formation of adiabatic shear instability [1, 4, 6, 31]. The ability of a cold sprayed particle to undergo plastic deformation and adiabatic shear is a function of materials properties, such as yield strength and melting point as well as process conditions, such as deposition temperature, particle velocity and particle size [4, 6, 7, 32]. When a particle arrives at the substrate at its critical velocity, there is good chance that adiabatic shear will take place, which will then contribute to a formation of a metallurgical bonding [3, 10]. However, even when a coating is created with average in-flight particle velocity well above the critical velocity, incomplete bonding is often observed [8, 11, 33]. This is especially true for materials with high melting point and high yield strength, like Ti and its alloys [6].

The cold spray process is somewhat complex and the effects of particle or substrate characteristics, temperature, gas flow and the nozzle design on the quality of cold spray deposits are not easy to evaluate using experimental methods. Many studies instead make use of computational simulations [2, 3, 6, 20]. The technique used here measures bond strength at the splat level, which is the level where the basic mechanism of adiabatic shear instability takes place. Identification of the effect of processing parameters on the underlying mechanism of adiabatic shear instability and the extent to which bonding occurs at the splat level is one simple

way to attempt optimization of the process to achieve the best coatings possible. The splat adhesion test [8] is a very useful experimental method that can directly address the effect of the process conditions on bonding of cold spray splats. Thus, process parameters of the cold spray process can be explored without spraying large quantities of material to identify the best conditions leading to sufficient adiabatic shear for a formation of a continuous and strong bonding.

4.1 - Effect of process conditions

One important processing consideration is the effect of non-uniform distribution of velocity across the gas jet. Many simulations have indicated that particle velocity is not continuous and varies depending on the particle position in the gas jet [20, 34, 35]. Zahiri et al. demonstrated that the particles traveling at the center of the gas jet had a higher particle velocity when compared to the particles traveling at the edge of the gas jet [20, 35]. The adhesion test of the splats carried in the present study showed that particles deposited at the edges of the gas jet had lower adhesion (~ 20 – 100 MPa) compared to those arriving in near the center of the jet (~ 200 MPa), as was seen in Fig. 12. This effect was likely due to the drop-off in the velocity as one moves away from the center of the jet. The poor adhesion strength of particles at the edges of the gas jet can affect the mechanical integrity of the cold spray coatings. To optimize deposition of hard to deposit materials, such as Ti and Ti6Al4V, a better design of the nozzle may be required [1, 34]. In one work, the use of a rectangular nozzle provided a more homogenous velocity distribution across the gas jet when compared to the circular nozzle [1]. If in the future, high quality cold sprayed coatings of high temperature, high strength materials are to be realized, nozzle design and optimization of the gas flow will be significant contributions leading to success in this endeavour.

Feedstock particle size is another important processing parameter as different particle sizes lead to different velocities [2, 6, 29]. Assuming one has already chosen an optimum range of particle sizes, within this size range, small particles travel at higher velocities than larger particles. At the same time the ability of smaller particle to undergo adiabatic shear is reduced and higher velocities are often required in order to deposit smaller particles when compared to particles of larger size [2, 6]. The results from splat adhesion test showed that for Ti, the adhesion strength for smaller particles was higher when compared to larger particles. Particles with diameters of 15 μm or less had adhesion of roughly 300 MPa, while those with diameter surpassing 40 μm had adhesion on the order of 200 MPa. The ratio of the deposition velocity vs. critical velocity of smaller particles was, therefore, higher than for the larger particles. It is important to note that the particles analysed in this study ranged from 10 to 60 μm and were tested at the center of the deposition pass. At this range, the effect of the particle size may not have played a substantial role on the adiabatic shear and the bow shock effect [1], where small particles deviate from the deposition trajectory, was not taken into account. Furthermore, the particles were deposited directly on the annealed substrate material. The effect of particle size on the particle bonding mechanisms in the coating subjected to high stress may be different [6, 21]. Additional studies on the particle size effect on the deposition efficiency and structural integrity of Ti and Ti6Al4V cold spray coating are needed.

The material composition had a significant effect on cold spray deposition. The adhesion strength of Ti splats deposited on Ti was consistently higher than the adhesion strength of Ti6Al4V splats deposited on Ti6Al4V substrate. This behavior can be explained by a

significantly higher yield strength of Ti6Al4V at 1200 MPa when compared to that of pure Ti at 700 MPa [36]. The yield strength of the material affects the critical velocity required to induce adiabatic shear in the material and therefore the ability of the material to form a strong, metallurgical bond [4, 6].

For cold spray, increasing temperature has a beneficial effect on the yield strength of the sprayed material [37]. The gas interaction with the feed-stock powder and substrate as well as the particle impact with the substrate can increase the temperature both locally and globally [1-3, 30]. According to Schmidt et al., using calculations done for copper particles, the particle temperature can reach up to 200°C in the gas preheated to 600 °C [2]. With increase in the temperature, the shear stress of the Ti6Al4V subjected to high strain rates decreases [37] and therefore contribute to an earlier onset of adiabatic shear instability and material bonding. Figure 7b indicates that a slight increase in the adhesion strength (~50 MPa) was measured for Ti6Al4V splats deposited on Ti6Al4V substrate with nitrogen gas preheated to a higher temperature than with helium gas under same deposition velocity but at lower gas preheat temperature. The shear stress in pure Ti is lower than that of its alloy, and the effect of the gas preheat temperature on particle adhesion was less noticeable, see Figure 7a. During the deposition of the individual cold spray splats, the gas interaction with the substrate material was limited, however, it is important to note that gas temperature can increase the substrate temperature given enough time [1]. J.-G. Legoux et al. used infrared camera and measured the temperature of 330°C in substrate region subjected to a stationary impact with nitrogen gas preheated to 500°C [30]. For Ti6Al4V, such increase in the temperature can significantly affect the deformation and adhesion mechanisms of the material [37].

To evaluate the effect of the substrate temperature on the deposition of the cold spray splats, Ti and Ti6Al4V splats were deposited on Ti or Ti6Al4V substrates preheated to 400°C. An increase of over 100 MPa in adhesion strength was measured in both cases. Furthermore, near ideal shearing behaviour, Regime 3 behavior, was observed for Ti splats deposited at 825 m/s on preheated Ti substrate as opposed to 1140 m/s in case of an unheated substrate. Ti6Al4V splats also demonstrated an improvement in the splat adhesion behaviour. Ti6Al4V splats deposited at 834 m/s on preheated Ti6Al4V substrate were shearing according to the Regime 2 whereas same splats deposited on unheated substrate were shearing according to Regime 1. In Regime 2 shearing behaviour material demonstrates regions with a ductile fracture, shown in Figure 9, which is indicative of a partial metallurgical bonding, whereas in Regime 1, the particles adhered mainly through a weaker conformal adhesion.

While a good correlation is found between the splat adhesion strength and splat shearing behavior, the splat deformation behavior does not follow same rules. The flattening ratio does not reflect the drastic increase in the splat adhesion strength seen in Ti splats deposited with helium gas in Figure 7a and on preheated substrates in Figure 14. The results indicate that the splat flattening ratio is not a good measure of the impact stresses, adiabatic shear and bonding, and that there are other parameters, such as: strain rate, stress localization, temperature and substrate deformation that have to be considered.

4.2 –Splat adhesion testing and literature comparisons

The splat adhesion test technique is one of the few techniques available testing that can measure the bonding mechanisms in the individual cold spray splats as the splat shearing takes place. The information can be used to define the strength, the type and the continuity of the

bonded interface between splat and substrate material. Up to date, this splat shearing technique was applied in the study of the adhesion strength of titanium splats on Ti coatings [8] and, a similar method was used on TiO_2 ceramic cold spray splats on stainless steel substrates [38]. It was also used in a recent study of the cohesive strength of cold spray Ti coatings, where a good correlation was found between the splat adhesion and particle cohesion strength in the coatings [24]. Another method of splat adhesion testing was developed by Guetta et al., called LASAT or laser shock adhesion test, They used it to measure the adhesion strength of individual cold spray copper splats embedded in the aluminum substrate [9].

Other adhesion testing techniques used today are always much more macroscopic. These include a hydraulic adhesion/tensile test (PAT, DFD Instruments, Kristiansand, Norway). In hydraulic adhesion/tensile test, the coating is typically glued to two circular elements with heat cured epoxy that are then pulled apart thus shearing coating from the substrate [3, 39]. Hydraulic adhesion/tensile test was used by T. S. Price et al. to measure the bond strength of Ti coating deposited on as-received and grit blasted Ti6Al4V substrate [39]. The coatings were deposited at 500 m/s and the bond strength was measured to be 32 - 37 MPa [39]. Morrocco et al. measured the bond strength of Ti coatings on the polished, grit blasted and ground Ti6Al4V substrates, and measured the adhesion strength between 5 and 25 MPa [40]. G. Bae et al., measured the bond strength of Ti coatings deposited at 650 m/s on steel substrate [3]. The adhesion strength on Ti coatings deposited on mild steel was measured to be between 49 and 69 MPa. In most cases, the failure occurred in the epoxy, failing at 85 MPa, and the bond strength of the coatings deposited at higher deposition velocities then the ones reported was not performed [3, 39].

The tubular coating tensile (TCT) test is a more commonly used technique to measure the cohesion strength of particles in the coating. The method was first developed by Schmidt et al. for the measurement of the cohesive strength of copper cold spray particles in the coating deposited on the aluminum substrate [2] but was later implemented in studies on other materials [18]. Binder et al. used TCT test and measured the cohesive strength of cold sprayed Ti particles in the coating deposited with nitrogen gas at 600°C to 1000°C to be between 100 and 300 MPa [18]. The coatings were deposited with a Kinetic 8000 Cold Spray Gun and Ti powder with 33.5 μm average diameter. The deposition velocities were not measured but were calculated to range between 650 and 800 m/s for 25 μm particles [18]. A good correlation was found between the particle cohesion in Ti coating obtained by Binder et al. and splat adhesion tests carried in this study. In Figure 17, the cohesion results obtained by Binder et al., were superposed on the results obtained using the splat adhesion test. For simplicity, the adhesion results were plotted as a function of the Ti splat and coating deposition velocity obtained with nitrogen gas only. The literature results on Ti particle cohesion strength correlate well with the adhesion strength of Ti splats measured with the modified ball bond shear technique. At deposition velocities above 700 m/s the adhesion strength of Ti splats deposited on the preheated Ti substrates correlated better with the literature results on the cohesive strength of Ti particles in the coatings. The cohesion strength of particles in the coating was most likely affected by an increase in the substrate material temperature following the high velocity impact of high temperature gas and particles.

Splat adhesion testing technique was shown to give a good approximation as to the deposition behavior and adhesion of the splats in the coating at any deposition velocity. The small scale precision of the method was ideal for tracking the effect of gas temperature, particle size and the particle position in the gas jet on the adhesion strength of splats which are hard to define using more conventional techniques. There are, however, a number of limitations in the current technique. The adhesion testing cannot be carried on the splats deposited on top of very

rough substrates since the roughness of the substrate contributes to the noise in the measurements. Splats that are imbedded in the substrate cannot be tested. In cases when the splats were found to be 40% imbedded in the substrate, the adhesion strength measurements were underestimated by roughly 7%. Current study did not test the cohesion strength of particles inside of the coating, however publication on this topic already exist [41] and would be a subject for upcoming studies. Future studies are also required to understand the stress distribution in the splat upon the splat shearing and would require finite element analysis.

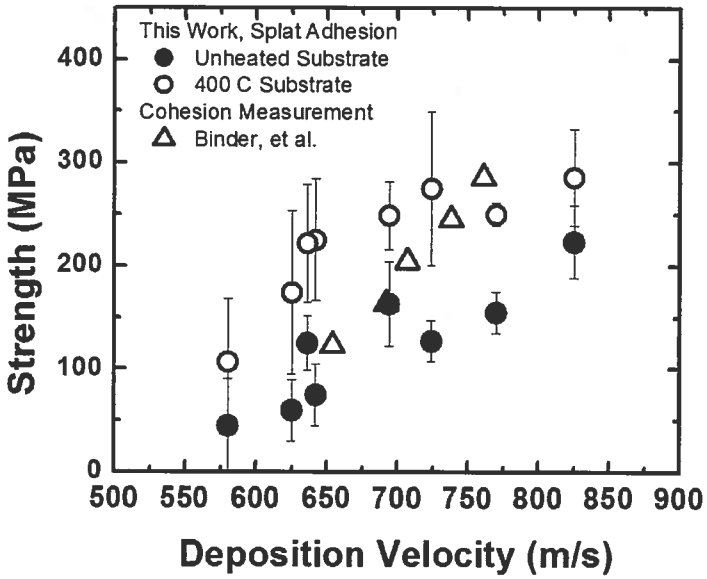

Figure 17: Literature comparison of adhesion and cohesion strength of cold spray coatings with the adhesion strength of cold spray splats measured on as-received and on preheated substrates.

Conclusion

A splat adhesion testing technique was used to test the effect of the deposition velocity, gas temperature, substrate temperature and particle size on the adhesion strength of Ti and Ti6Al4V splats deposited on Ti or Ti6Al4V substrates. Strong adhesion strength approaching the theoretical shear strength (at 380MPa) was measured for Ti splats deposited on Ti substrates at velocities significantly higher (at 1140 m/s) than the critical velocity for that material. Ti6Al4V splats deposited on Ti6Al4V substrate demonstrated poor particle adhesion and a bonded interface that was not fully continuous, with only traces of metallurgical bonding, even at 1115 m/s.

An increase in the adhesion strength of splats was measured after the preheating of the Ti and Ti6Al4V substrates to 400°C. Ideal shearing behavior with fully bonded splat/substrate interface and adhesion strength of 284 MPa was measured for Ti deposited at 825 m/s on preheated substrates. A significant improvement in the adhesion strength was also observed for Ti6Al4V splats deposited on preheated Ti6Al4V substrates. A combination of high velocities, preheating of the powder and substrate may be a key to the deposition of Ti6Al4V splats with near theoretical adhesion strength,

The adhesion strength of splats was found to vary with particle size and particle position in the deposition pass. Particle deposited at the center of the deposition pass and of smaller particle diameter showed superior adhesion strength when compared to the large particles or particles at the edge of the deposition pass.

The extent of particle deformation measured in terms of splat flattening ratio, did not reflect well the degree of splat adhesion, and was found to be a poor measure of the onset of adiabatic shear and bonding. The deformation of the substrate, on the other hand, was found to have a beneficial effect on the particle adhesion attributed to a confinement of the adiabatic shear region within the splat/substrate interface leading to a more successful metallurgical bonding.

The splat adhesion results correlated well with the cohesion strength of particles in the coating. The modified ball bond shear technique can, therefore, provide a comprehensive and a low cost approach for optimization of cold spray deposition parameters.

Acknowledgement

The cold spray equipment was provided by CFI project No. 8246, McGill University. The authors acknowledge the technical assistance of Bernard Harvey, Mario Lamontagne, Jean-Francois Alarie and Frederic Belval. The authors would also like to thank Jolanta Klemberg Sapieha from Ecole Polytechnique for access to CSM Instrument.

References

1. A. Papyrin, V. Kosarev, K.V. Klinkov, A. Alkhimov, and V.M. Fomin, Cold Spray Technology, A. Papyrin. Ed., Elsever, 2006.
2. T. Schmidt, F. Gaertner, and H. Kreye, New developments in cold spray based on higher gas and particle temperatures, *Journal of Thermal Spray Technology*, 2006, **15** (4), p. 488-494
3. G. Bae, S. Kumar, S. Yoon, K. Kang, H. Na, H.J. Kim, and C. Lee, Bonding features and associated mechanisms in kinetic sprayed titanium coatings, *Acta Materialia*, 2009, **57** (19), p. 5654-5666, in English
4. H. Assadi, F. Gärtner, T. Stoltenhoff, and H. Kreye, Bonding mechanism in cold gas spraying, *Acta Materialia*, 2003, **51** (15), p. 4379-4394
5. M. Grujicic, C.L. Zhao, W.S. DeRosset, and D. Helfritch, Adiabatic shear instability based mechanism for particles/substrate bonding in the cold-gas dynamic-spray process, *Materials & Design*, 2004, **25** (8), p. 681-688
6. T. Schmidt, F. Gärtner, H. Assadi, and H. Kreye, Development of a generalized parameter window for cold spray deposition, *Acta Materialia*, 2006, **54** (3), p. 729-742
7. D. Goldbaum, R.R. Chromik, S. Yue, E. Irissou, and J.-G. Legoux, Mechanical property mapping of cold spray Ti splats, *Journal of Thermal Spray Technology*, 2011, **20**, p. 486-496
8. R.R. Chromik, D. Goldbaum, J.M. Shockley, S. Yue, E. Irissou, J.-G. Legoux, and N.X. Randall, Modified Ball Bond Shear Test for Determination of Adhesion Strength of Cold Spray Splats, *Surface & Coatings Technology*, 2010, **205** (5), p. 1409-1414
9. S. Guetta, M. Berger, F. Borit, V. Guipont, M. Jeandin, M. Boustie, Y. Ichikawa, K. Sakaguchi, and K. Ogawa, Influence of Particle Velocity on Adhesion of Cold-Sprayed Splats, *Journal of Thermal Spray Technology*, 2009, **18** (3), p. 331-342
10. J. Vlcek, H. Huber, H.F. Voggenreiter, and E. Lugscheider, Melting upon particle impact in the cold spray process, *International Congress on Advanced Materials, Their Process and Applications*, 2002.

11. G. Bae, Y. Xiong, S. Kumar, K. Kang, and C. Lee, General aspects of interface bonding in kinetic sprayed coatings, *Acta Materialia*, 2008, **56** (17), p. 4858-4868
12. R. Kapoor, and S. Nemat-Nasser, Determination of temperature rise during high strain rate deformation, *Mechanics of Materials*, 1998, **27** (1), p. 1-12
13. S. Guetta, M.H. Berger, F. Borit, V. Guipont, M. Jeandin, F. Evry, M. Boustie, F. Poitiers, Y. Ichikawa, K. Ogawa, and J. Sendai, Influence of particle velocity on adhesion of cold-sprayed splats, *Thermal Spray Conference & Exposition: Thermal Spray Crossing Borders*, ASM International, 2008, p. 726-731.
14. C. Borchers, F. Gartner, T. Stoltenhoff, and H. Kreye, Microstructural bonding features of cold sprayed face centered cubic metals, *Journal of Applied Physics*, 2004, **96** (8), p. 4288-4292
15. T. Hussain, D. McCartney, P. Shipway, and D. Zhang, Bonding Mechanisms in Cold Spraying: The Contributions of Metallurgical and Mechanical Components, *Journal of Thermal Spray Technology*, 2009, **18** (3), p. 364-379
16. K. Kim, M. Watanabe, J. Kawakita, and S. Kuroda, Effects of Temperature of In-flight Particles on Bonding and Microstructure in Warm-Sprayed Titanium Deposits, *Journal of Thermal Spray Technology*, 2009, **18** (3), p. 392-400
17. E. Irissou, J.G. Legoux, C. Moreau, and A.N. Ryabinin, How cold is cold spray? An experimental study of the heat transfer to the substrate in cold gas dynamic spraying, *International Thermal Spray Conference & Exposition: Thermal Spray Crossing Borders*, Jun 2-4, 2008 (City), [insert publication year].
18. K. Binder, J. Gottschalk, M. Kollenda, F. Gärtner, and T. Klassen, Influence of Impact Angle and Gas Temperature on Mechanical Properties of Titanium Cold Spray Deposits, *Journal of Thermal Spray Technology*, 2010, p. 1-9
19. P.C. King, and M. Jahedi, Relationship between particle size and deformation in the cold spray process, *Applied Surface Science*, 2010, **256** (6), p. 1735-1738
20. S. Zahiri, W. Yang, and M. Jahedi, Characterization of Cold Spray Titanium Supersonic Jet, *Journal of Thermal Spray Technology*, 2009, **18** (1), p. 110-117
21. W. Wong, A. Rezaeian, E. Irissou, J.G. Legoux, and S. Yue, Cold spray characteristics of commercially pure Ti and Ti-6Al-4V, *Advanced Materials Research*, 2010, **89-91**, p. 639-644
22. G.F. Vander Voort, Metallography, principles and practice, ASM International, 1999.
23. W.C. Oliver, and G.M. Pharr, An improved technique for determining hardness and elastic modulus using load and displacement sensing indentation experiments *J. Mater. Res.*, 1992, **7** (6), p. 1564-1583
24. D. Goldbaum, J. Ajaja, R.R.W. Chromik, W. , S. Yue, and E.L. Irissou, J.-G., Mechanical Behavior of Ti Cold Spray Coatings Determined by a Multi-Scale Indentation Method, submitted to *Journal of Materials Science and Engineering A*, 2010.
25. Materials Property Handbook: Titanium Alloys, ASM International.
26. G. Lutjering, and J.C. Williams, Titanium, Springer, 2003.
27. V.A. Joshi, Titanium Aloys An Atlas of Structures and Fracture Features, CRC Taylor & Francis Group, 2006.
28. E. Irissou, J.-G. Legoux, A. Ryabinin, B. Jodoin, and C. Moreau, Review on Cold Spray Process and Technology: Part I—Intellectual Property, *Journal of Thermal Spray Technology*, 2008, **17** (4), p. 495-516
29. B. Samareh, and A. Dolatabadi, A Three-Dimensional Analysis of the Cold Spray Process: The Effects of Substrate Location and Shape, *Journal of Thermal Spray Technology*, 2007, **16** (5), p. 634-642

30. J. Legoux, E. Irissou, and C. Moreau, Effect of Substrate Temperature on the Formation Mechanism of Cold-Sprayed Aluminum, Zinc and Tin Coatings, *Journal of Thermal Spray Technology*, 2007, **16** (5), p. 619-626
31. V.K. Champagne, The cold spray materials deposition process: Fundamentals and applications, Woodhead Publishing Limited, 2007.
32. C.-J. Li, W.-Y. Li, and H. Liao, Examination of the critical velocity for deposition of particles in cold spraying, *Journal of Thermal Spray Technology*, 2006, **15** (2), p. 212-222
33. K. Kim, M. Watanabe, K. Mitsuishi, K. Iakoubovskii, and S. Kuroda, Impact bonding and rebounding between kinetically sprayed titanium particle and steel substrate revealed by high-resolution electron microscopy, *Journal of Physics D: Applied Physics*, 2009, **42** (6), p. 65304
34. A. Alkhimov, V. Kosarev, and S. Klinkov, The features of cold spray nozzle design, *Journal of Thermal Spray Technology*, 2001, **10** (2), p. 375-381
35. V. Kosarev, S. Klinkov, A. Alkhimov, and A. Papyrin, On some aspects of gas dynamics of the cold spray process, *Journal of Thermal Spray Technology*, 2003, **12** (2), p. 265-281
36. J. Vlcek, L. Gimeno, H. Huber, and E. Lugscheider, A systematic approach to material eligibility for the cold-spray process, *Journal of Thermal Spray Technology*, 2005, **14** (1), p. 125-133
37. P. Follansbee, and G. Gray, An analysis of the low temperature, low and high strain-rate deformation of Ti–6Al–4V, *Metallurgical and Materials Transactions A*, 1989, **20** (5), p. 863-874
38. M.E. Dickinson, and M. Yamada, A New Method for Measuring Shear Adhesion Strength of Ceramic Cold Spray Splats, *Nanoscience and Nanotechnology Letters*, 2010, **2**, p. 348-351
39. T. Price, P. Shipway, and D. McCartney, Effect of cold spray deposition of a titanium coating on fatigue behavior of a titanium alloy, *Journal of Thermal Spray Technology*, 2006, **15** (4), p. 507-512
40. T. Marrocco, D. McCartney, P. Shipway, and A. Sturgeon, Production of titanium deposits by cold-gas dynamic spray: Numerical modeling and experimental characterization, *Journal of Thermal Spray Technology*, 2006, **15** (2), p. 263-272
41. G. Sundararajan, N. Chavan, G. Sivakumar, and P. Sudharshan Phani, Evaluation of Parameters for Assessment of Inter-Splat Bond Strength in Cold-Sprayed Coatings, *Journal of Thermal Spray Technology*, 2010, **19** (6), p. 1255-1266